Inorganic Chemistry

pubs.acs.org/IC Article

Phosphorescent Iridium(III) Complexes with a Dianionic C,C′,N,N′-Tetradentate Ligand

Llorenç Benavent, Pierre-Luc T. Boudreault, Miguel A. Esteruelas,* Ana M. López, Enrique Oñate, and Jui-Yi Tsai

Cite This: https://dx.doi.org/10.1021/acs.inorgchem.0c01377 Read Online

ACCESS | Metrics & More | Article Recommendations | Supporting Information

ABSTRACT: To prepare new phosphorescent iridium(III) emitters, 2-phenyl-6-(1-phenyl-1-(pyridin-2-yl)ethyl)pyridine (H_2L) has been designed and its reactions with $[Ir(\mu\text{-Cl})(\eta^4\text{-COD})]_2$ (**1**, COD = 1,5-cyclooctadiene) have been studied. The products obtained depend on the refluxing temperature of the solvent. Thus, complexes $Ir(\kappa^4\text{-}C,C',N,N'\text{-L})Cl(CO)$ (**2**), $[Ir(\eta^4\text{-COD})(\kappa^2\text{-}N,N'\text{-}H_2L)][IrCl_2(\eta^4\text{-COD})]$ (**3**), and $[Ir(\mu\text{-Cl})(\kappa^4\text{-}C,C',N,N'\text{-L})]_2$ (**4**) have been formed in 2-ethoxyethanol, propan-2-ol, and 1-phenylethanol, respectively. Complex **4** reacts with K(acac) to give the acetylacetonate derivative $Ir(\kappa^4\text{-}C,C',N,N'\text{-L})(acac)$ (**5**). Complexes **2** and **5** are efficient blue-green and green emitters of classes [6tt+1m+2m] and [6tt+3b], respectively. They display lifetimes in the range of 1.1−4.5 μs and high quantum yields (0.54−0.87) in both PMMA films and 2-MeTHF at room temperature.

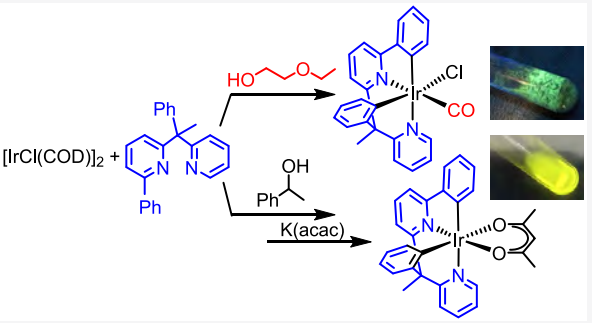

INTRODUCTION

Phosphorescent emitters based on iridium(III) display a rapid intersystem crossing from the lowest-lying singlet to the triplet excited states.[1] Thus, they are capable of harvesting both singlet and triplet excitons, which allows internal quantum efficiencies close to unity in their organic light-emitting diode (OLED) devices.[2] This ability of the iridium(III) complexes has situated their emitters at the forefront of the current photophysics.[3] The HOMO of these emitters comprises the metal and its associated ligands, whereas the LUMO is centered on π^* orbitals of some ligand. Thus, the HOMO−LUMO gap and the energy of the excited states may be governed by selecting their ligands. That is why there is a particular interest in emitters of this class bearing at least two different ligands.[4] The focus has been centered on derivatives containing two different types of 3e-donor bidentate ligands (3b and 3b′), commonly two orthometalated phenylpyridines and an acetylacetonate (acac). These [3b+3b+3b′] emitters are usually prepared through reactions of $[Ir(\mu\text{-Cl})(3b)_2]_2$ dimers with an acac salt.[5] A remarkable feature of these compounds is the mutually *trans* disposition of the pyridyl groups in their octahedral structures, with the notable exception of a few of them being stabilized by orthometalated fluorinated phenylpyridines.[6]

The use of pincer ligands has allowed the design of new families of phosphorescent emitters with promising applications for OLED fabrication, due to the high rigidity and stability enforced by their framework.[4a,j−l,7] The rigidity of the resulting molecular configuration has a positive effect on the thermally induced quenching because the nonradiative decay pathways are significantly suppressed, including the metal-centered d−d states.[8] Tetradentate ligands increase the strength of the metal−ligand binding, due to the interaction of the metal center with four electron-donor points of the ligand. Thus, they have been used as a tool to improve the phosphorescence quantum efficiency of d^8 metal complexes,[9] even of those displaying weaker spin−orbit coupling and thermally accessible metal-centered d−d states.[10] In addition, emitters with tridentate and tetradentate ligands give rise to fewer problems of isomers and reactions of redistribution than complexes stabilized by bidentate and monodentate ones, as a consequence of the decrease in the number of ligands attached to the metal for a given coordination index.

Tetradentate ligands with a planar skeleton have been the most commonly used,[11] while the photophysical properties of Ir(III) emitters with nonplanar ligands (Chart 1) have received scarce attention.[12] An increase in the phosphorescence efficiency has been attained by tethering the *ortho*-carboranes attached to the 5 positions of *ortho*-metalated 2-phenylpyridine ligands (complex **A**).[13] 2,7-Bis(2-(2-(4-(pyridin-2-yl)-phenoxy)ethoxy)ethoxy)naphthalene has been employed to

Received: May 11, 2020

https://dx.doi.org/10.1021/acs.inorgchem.0c01377
Inorg. Chem. XXXX, XXX, XXX−XXX

Chart 1. Ir(III) Emitters with Nonplanar Tetradentate Ligands

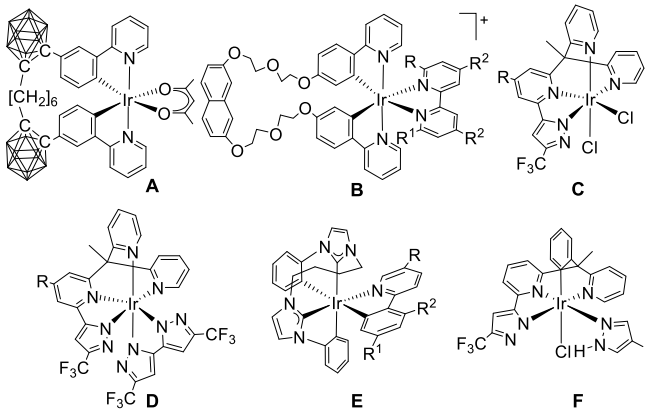

prepare cations **B**, to explore its use for white-light emission.[14] Hung, Chou, Chi, and co-workers have prepared 2,2′-(1-(6-pyrazol-5-yl)pyridin-2-yl)ethane-1,1-diyl)dipyridine molecules. These precursors afford monoanionic tetradentate ligands (7tt), which stabilize iridium(III) complexes of classes [7tt+1m+1m] and [7tt+2b] (**C** and **D**, respectively). Complexes **C** (R = H or ^{t}Bu) showed no perceptible emission. However, the substitution of the monodentate chlorides (1m) by a bipyrazolate ligand (2b), to give **D** (R = H or ^{t}Bu), produces a dramatic increase in the emission efficiency.[15] We have used 1,1-diphenyl-3,3-butylenediimidazolium iodide to prepare the [6tt+3b] emitters **E**, which display blue-green emissions with quantum yields close to unity.[16] Lee, Chi, and co-workers have recently replaced a peripheral pyridine in one of the organic molecules (R = H), previously prepared by the the group of Hung, Chou, and Chi, with a phenyl susceptible to *ortho*-C−H bond activation. The resulting dianionic tetradentate ligand (6tt) stabilizes mononuclear [6tt+1m+2m] (**F**) and binuclear emitters. The diiridium compounds exhibited bright sky-blue to green emission.[17]

In the search for Ir(III) emitters with a scaffold more rigid than those of type [3b+3b+3b′], we have designed 2-phenyl-6-(1-phenyl-1-(pyridin-2-yl)ethyl)pyridine, which is formed by moieties 2-phenylpyridine and pyridine attached to a 1-phenylethylidene linker by the *ortho* position of the pyridine rings (Chart 2). Our aim was to use it as a precursor of a

Chart 2. Dipyridine Precursor of the Tetradentate Ligand Used in This Work

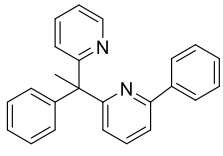

dianionic C,C′,N,N′-tetradentate ligand. The study of the reactions of this dipyridine with the [Ir(μ-Cl)(η^4-COD)]$_2$ dimer (**1**; COD = 1,5-cyclooctadiene), in different solvents, has led us to the discovery of new phosphorescent emitters of classes [6tt+1m+2m] and [6tt+3b]. This paper describes the preparation of new dipyridine phosphorescent iridium(III) compounds and their photophysical properties.

RESULTS AND DISCUSSION

Synthesis of the Dipyridine and the Emitters. 2-Phenyl-6-(1-phenyl-1-(pyridin-2-yl)ethyl)pyridine (H_2L) was prepared as a white solid in 50% yield by nucleophilic aromatic substitution of the fluoride substituent of 2-fluoro-6-phenylpyridine by the anion 1-phenyl-1-(pyridin-2-yl)ethan-1-ide, resulting from the deprotonation of the tertiary C(sp^3) atom of 2-(1-phenylethyl)pyridine (Scheme 1).

Scheme 1. Synthesis of 2-Phenyl-6-(1-phenyl-1-(pyridin-2-yl)ethyl)pyridine

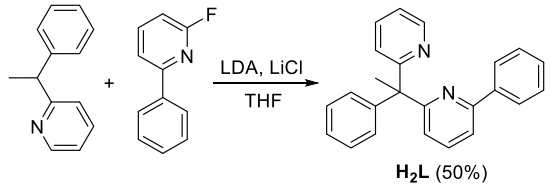

Having successfully obtained the organic precursor, we investigated its coordination to iridium(III). We were initially inspired by the procedure used to prepare emitters [3b+3b+3b′]. Thus, we tried to obtain an [Ir(μ-Cl)(6tt)]$_2$ dimer via the procedure commonly employed to generate the [Ir(μ-Cl)(3b)$_2$]$_2$ dimers, i.e., by means of the treatment of complex **1** with the chromophore, in 2-ethoxyethanol, under reflux, for 24 h. However, under these conditions, the reaction of **1** with H_2L led to the [6tt+1m+2m] carbonyl derivative Ir(κ^4-C,C′,N,N′-L)Cl(CO) (**2**; ν_{CO} = 2011 cm^{-1}, $\delta_{^{13}C}$ 172.4), which was obtained as a pale yellow solid in 59% yield (Scheme 2).

Scheme 2. Preparation of Compounds 2−5, Including Isolated Yields with Respect to 1

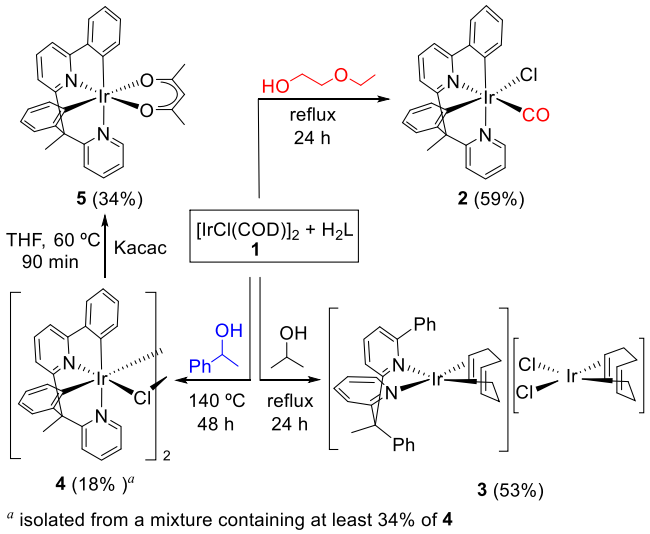

[a] isolated from a mixture containing at least 34% of **4**

Complex **2** was characterized by X-ray diffraction analysis. Figure 1 gives a view of the molecule. The structure proves the coordination of both pyridines, the *ortho*-C−H bond activation of both phenyl groups, and the presence of the carbonyl ligand. Furthermore, it reveals a mutually *cis* disposition of the pyridine groups [N(1)−Ir−N(2) angle of 89.5(2)°], which is in contrast to that observed in emitters with two *ortho*-metalated 2-phenylpyridines. The coordination polyhedron around the iridium atom can be rationalized as a distorted

https://dx.doi.org/10.1021/acs.inorgchem.0c01377
Inorg. Chem. XXXX, XXX, XXX−XXX

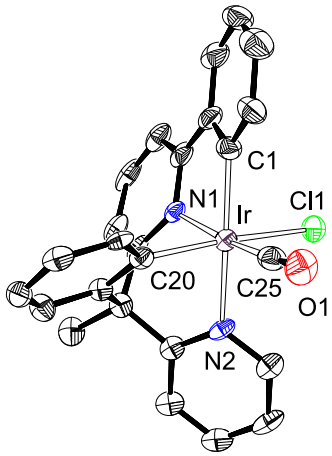

Figure 1. X-ray structure of **2** (50% probability ellipsoids). Hydrogen atoms are omitted for clarity. Selected bond lengths (angstroms) and angles (degrees): Ir−C(1), 2.018(8); Ir−C(20), 2.031(7); Ir−N(1), 2.042(6); Ir−N(2), 2.144(6); Ir−Cl(1), 2.4534(19); C(1)−Ir−N(2), 167.2(3); C(25)−Ir−N(1), 171.6(3); C(20)−Ir−Cl(1), 168.8(2); N(1)−Ir−N(2), 89.5(2); C(1)−Ir−C(20), 98.7(3) (50% probability ellipsoids). Hydrogen atoms have been omitted for the sake clarity.

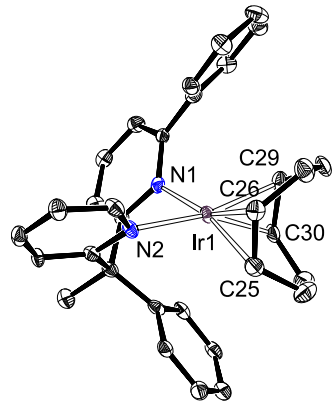

Figure 2. X-ray structure of the cation of **3** (50% probability ellipsoids). Hydrogen atoms are omitted for clarity. Selected bond lengths (angstroms) and angles (degrees): Ir(1)−N(1), 2.137(5); Ir(1)−N(2), 2.107(4); Ir(1)−C(25), 2.134(6); Ir(1)−C(26), 2.125(6); Ir(1)−C(29), 2.144(6); Ir(1)−C(30), 2.137(6); N(2)−Ir(1)−N(1), 81.00(17) (50% probability ellipsoids). Hydrogen atoms have been omitted for the sake clarity.

octahedron with the metalated phenyl group of the 2-phenylpyridine moiety in the *trans* position with respect to the other pyridine ring [C(1)−Ir−N(2) angle of 167.2(3)°]. At the perpendicular plane, the metalated phenyl group attached to the C(sp^3) atom is situated *trans* to the chloride anion [C(20)−Ir−Cl(1) angle of 168.8(2)°], whereas the carbonyl ligand lies *trans* to the pyridine ring of the 2-phenylpyridine unit [C(25)−Ir−N(1) angle of 171.6 (3)°].

The source of the carbonyl ligand of **2** is the reaction solvent. The ability of iridium to promote the dehydrogenation of primary alcohols to the corresponding aldehydes,[18] which undergo metal-promoted decarbonylation, to afford carbonyl derivatives is well-known.[19] To prevent the carbonylation of the metal center, we changed 2-ethoxyethanol to a secondary alcohol, 2-propanol, and repeated the reaction under refluxing conditions. In this case, the desired $[Ir(\mu\text{-Cl})(6tt)]_2$ dimer was not obtained; instead, the orange salt $[Ir(\eta^4\text{-COD})(\kappa^2\text{-}N,N'\text{-}H_2L)][IrCl_2(\eta^4\text{-COD})]$ (**3**) precipitated (53%). The new compound was also characterized by X-ray diffraction analysis. Figure 2 shows the structure of the cation, which displays the expected square-planar arrangement of ligands around the iridium center with the dipyridine acting as a chelate [N(1)−Ir−N(2) angle of 81.00(17)°]. The coordinated olefinic bonds have lengths of 1.410(8) Å [C(25)−C(26)] and 1.390(8) Å [C(29)−C(30)], which are longer than the C═C bonds in the free diolefin (1.34 Å)[20] as expected for the usual Dewar−Chatt−Duncanson model. In dichloromethane, the dipyridine exchanges its position between the Ir(η^4-COD) moieties of the cation and the anion, even at 193 K. The process appears to take place by dissociation of the dipyridine and the subsequent coordination to the other metal center, according to the ^{1}NMR spectra of the salt that show signals characteristic of **1** and the free ligand in addition to very broad resonances.

The formation of **3** reveals that the refluxing temperature of 2-propanol (83 °C) is not enough to reach the *ortho*-C−H bond activation of the phenyl groups of the chromophore. Then, we came back to repeat the reaction using 1-phenylethanol as the solvent, which is also a secondary alcohol but has a boiling point of 204 °C. This time, a complex mixture was formed. Its treatment with dichloromethane yielded an orange solid (18%), which fortunately corresponded to the $[Ir(\mu\text{-Cl})(\kappa^4\text{-}C,C',N,N'\text{-L})]_2$ dimer (**4**), according to its C,H,N-elemental analysis and MALDI-TOF spectrum ($[M/2]^+$ 562.0). This slight success encouraged us to directly treat the mixture with K(acac) in tetrahydrofuran, for 1.5 h, at 60 °C. After the purification of the reaction crude by silica column chromatography, the target complex Ir(κ^4-*C,C',N,N'*-L)(acac) (**5**) was obtained as a yellow solid, in 34% yield with respect to **1**. The formation of **5** was confirmed by X-ray diffraction analysis. The structure (Figure 3) shows the same arrangement

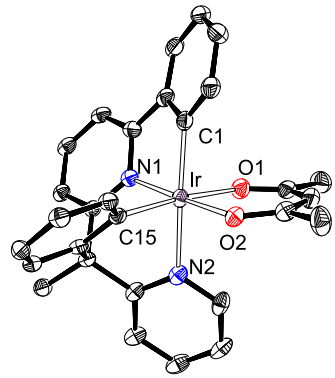

Figure 3. X-ray structure of **5** (50% probability ellipsoids). Hydrogen atoms are omitted for clarity. Selected bond lengths (angstroms) and angles (degrees): Ir−C(1), 1.996(5); Ir−C(15), 1.991(5); Ir−N(1), 1.976(4); Ir−N(2), 2.110(4); Ir−O(1), 2.148(4); Ir−O(2), 2.058(4); C(1)−Ir−N(2), 169.15(18); N(1)−Ir−O(2), 175.98(15); C(15)−Ir−O(1), 172.22(16); N(1)−Ir−N(2), 92.19(16); C(1)−Ir−C(15), 101.63(19) (50% probability ellipsoids). Hydrogen atoms have been omitted for the sake clarity.

of the tetradentate ligand as in **2** [N(1)−Ir−N(2) angle of 92.19(16)° and C(1)−Ir−N(2) angle of 169.15(18)°]. Thus, the coordination polyhedron around the iridium atom can be rationalized as the expected octahedron with O(1)−Ir−C(15) and O(2)−Ir−N(1) angles of 172.22(16)° and 175.98(15)°, respectively.

https://dx.doi.org/10.1021/acs.inorgchem.0c01377
Inorg. Chem. XXXX, XXX, XXX−XXX

Photophysical and Electrochemical Properties of Complexes 2 and 5. The ultraviolet−visible (UV−vis) spectra of 2-methyltetrahydrofuran (2-MeTHF) solutions of these compounds are similar (Figure 4 and Figures S1 and S2).

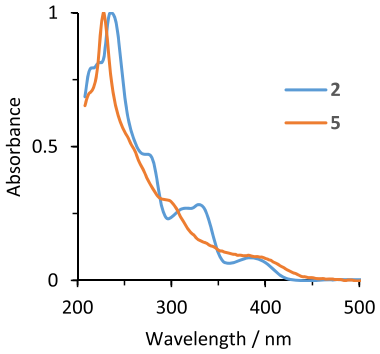

Figure 4. UV−vis absorption spectra of complexes **2** and **5** recorded in a 2-MeTHF solution (1.0×10^{-4} M) at 298 K.

Selected absorption data are listed in Table 1. For both complexes, the main absorptions may be placed in three groups: <320, 320−430, and >430 nm. Time-dependent density functional theory (DFT) calculations [tetrahydrofuran, B3LYP-GD3//SDD(f)/631G**] indicate that the absorptions of the highest energy should be assigned to $^1\pi-\pi^*$ intra- and interligand transitions, whereas those between 320 and 430 nm are due to spin-allowed Ir-to-6tt charge transfer (^{1}MLCT) mixed with 6tt-to-6tt (ILCT, for **2** and **5**) and acac-to-6tt (LLCT, for **5**) transitions (Table 1 and Tables S1−S4). The absorption tails after 430 nm correspond to formally spin-forbidden ^{3}MLCT transitions, which are produced by the large spin−orbit coupling introduced by the iridium center with some contribution from the $^3\pi-\pi^*$ transitions.

The electrochemical behavior of **2** and **5** was also investigated to gain more insight into their frontier molecular orbitals. The study was performed using cyclic voltammetry in a degassed acetonitrile solution, under argon, and the potentials are reported versus Fc/Fc$^+$. The results are listed in Table 2 and shown in Figure S3. Complex **2** shows an irreversible oxidation at 1.11 V, whereas **5** exhibits a quasi-reversible oxidation at 0.42 V. However, no reduction peaks were observed within the solvent window for any of the compounds. Experimental HOMO levels calculated from the respective oxidation potentials compare well with those computed: −5.91 versus −5.71 eV for **2** and −5.22 versus −5.05 eV for **5** (Tables S5 and S6 and Figures S4−S6). The lower oxidation potential of **5** is consistent with its higher HOMO energy level. The computed HOMO−LUMO gaps are 3.98 eV for **2** and 3.71 eV for **5**. The latter is similar to that found for complexes Ir{κ^2-*C*,*N*-[C_6H_3R-py]}{κ^2-*C*,*N*-[C_6H_4-py]}(acac) (R = Br, Me, or Ph)[21] and Ir{κ^2-*C*,*C*-[C_6H_4-ImMe]}{κ^2-*C*,*N*-[$C_6H_2R_2$-py]}(acac) (R = H or F),[22] which display similar oxidations in the range of 0.36−0.51 V and have no reduction peaks.

Table 2. Electrochemical and DFT MO Energy Data for Complexes 2 and 5

		obs (eV)	calcd (eV)		
complex	E^{ox}[a] (V)	HOMO[b]	HOMO[c]	LUMO[c]	HLG[c]
2	1.1[d]	−5.91	−5.71	−1.73	3.98
5	0.42[e]	−5.22	−5.05	−1.34	3.71

[a]Measured under argon in an acetonitrile/[Bu_4N]PF_6 (0.1 M) mixture, vs Fc/Fc$^+$. [b]HOMO = −(E^{ox} vs Fc/Fc$^+$ + 4.8) eV. [c]Values from DFT calculations. [d]Anodic potential (irreversible oxidation). [e]$E_{1/2}{}^{ox}$ (quasi-reversible oxidation).

Complexes **2** and **5** are phosphorescent emitters upon photoexcitation, in doped poly(methyl methacrylate) (PMMA) at 5 wt % and room temperature and in 2-MeTHF at room temperature and 77 K (Figure 5 and Figures S7−S12). The former is blue-green emissive (468−508 nm), whereas the latter is green (527−562 nm) (Table 3). The difference is consistent with the computed HOMO−LUMO gap, smaller for **5** than for **2**. The emission spectra of **5** at room temperature exhibit broad bands, whereas those of **2** display vibronic structures according to panels a and b of Figure 5. The spectra in 2-MeTHF at 77 K of both compounds display

Table 1. Selected UV−Vis Absorptions for 2 and 5

λ_{exp}[a] (nm)	ε[a] (M^{-1} cm^{-1})	excitation energy[b] (nm)	oscillator strength[b]	transition[b]	character of the transition[b]
			Complex Ir(κ^4-*C*,*C*′,*N*,*N*′-L)Cl(CO) (**2**)		
236	12160	232	0.0891	HOMO → LUMO+9 (19%)	ILCT/LLCT (6tt → 6tt + CO)
				H-4 → L+3 (14%), H-2 → L+5 (10%)	ILCT/LLCT (6tt + Cl → 6tt + CO)
274	5730	273	0.0237	HOMO → LUMO+5 (79%)	ILCT/LLCT (6tt → 6tt + CO)
316	3280	312	0.0702	HOMO−2 → LUMO (66%)	ILCT/LLCT (6tt + Cl → 6tt)
330	3440	329	0.0258	HOMO → LUMO+1 (93%)	MLCT/ILCT (Ir + 6tt → 6tt)
384	1030	385 (S_1)	0.0249	HOMO → LUMO (98%)	MLCT/ILCT (Ir + 6tt → 6tt)
476	40	443 (T_1)	0	HOMO → LUMO (53%)	^{3}MLCT/^{3}ILCT (Ir + 6tt → 6ttt)
			Complex Ir(κ^4-*C*,*C*′,*N*,*N*′-L)(acac) (**5**)		
228	5730	239	0.0159	HOMO−5 → LUMO+4 (41%)	ILCT (6tt → 6tt)
258	2880	259	0.1275	HOMO → LUMO+7 (55%)	MLCT/ILCT (Ir + 6tt → 6tt)
294	1730	298	0.175	HOMO−3 → LUMO (48%)	ILCT (6tt → 6tt)
344	730	363	0.0481	HOMO−1 → LUMO+1 (86%)	MLCT/ILCT/LLCT (Ir + 6tt + acac → 6tt)
408	400	426 (S_1)	0.0145	HOMO → LUMO (88%)	MLCT/ILCT (Ir + 6tt → 6tt)
462	40	476 (T_1)	0	HOMO−1 → LUMO (52%)	^{3}MLCT/^{3}ILCT/^{3}LLCT (Ir + 6tt + acac → 6tt)
				HOMO → LUMO (27%)	^{3}MLCT/^{3}ILCT (Ir + 6tt → 6tt)

[a]In 2-MeTHF. [b]Computed TD-DFT in THF.

https://dx.doi.org/10.1021/acs.inorgchem.0c01377
Inorg. Chem. XXXX, XXX, XXX−XXX

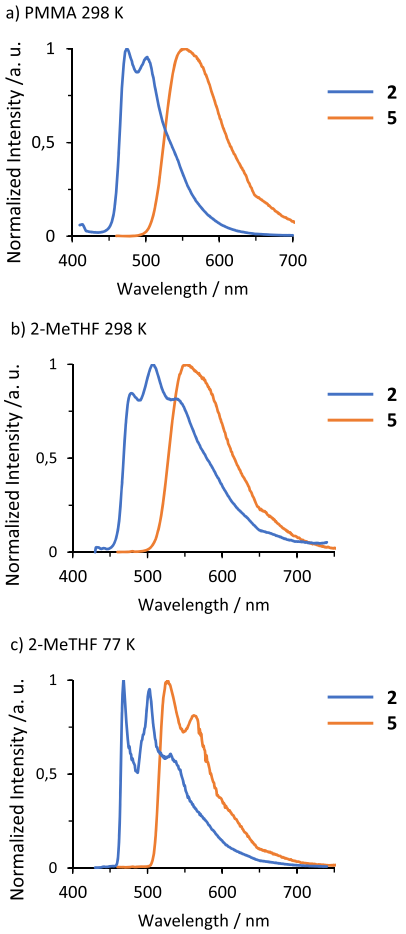

Figure 5. Emission spectra of **2** and **5** in (a) 5 wt % PMMA films at 298 K, (b) 2-MeTHF at 298 K, and (c) 2-MeTHF at 77 K.

vibronic fine structures. According to panels b and c of Figure 5, and a spin density plot (Figure 6), it appears that complex **2** has a dominating ligand-centered ^{3}LC state, while complex **5** is contributed by an admixture of metal to ligand charge transfer (^{3}MLCT) and ligand-centered (^{3}LC) states. The emissions can be attributed to T_1 excited states, which originate mainly by charge transfer transitions between HOMO → LUMO (**2**) and HOMO−1 → LUMO and HOMO → LUMO (**5**). Thus, there is good agreement between the experimental emission wavelengths and those calculated by estimating the difference in energy between the optimized T_1 and S_0 states, in tetrahydrofuran (Table 3). The lifetimes (τ = 1.1−4.5 μs) are short and similar for both emitters. At room temperature, the quantum yield (Φ) of **2** in PMMA (0.87) is significantly higher than in 2-MeTHF (0.54); accordingly, the ratio between the radiative (k_r) and nonradiative (k_{nr}) rate constants

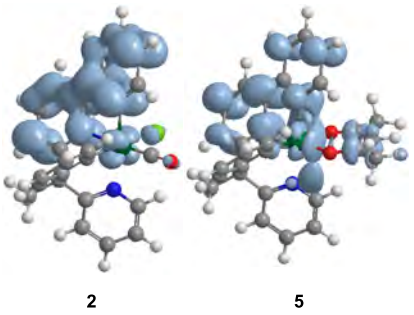

Figure 6. DFT-calculated spin density of **2** and **5** at 0.002 au contour levels for the T_1 excited state.

is >5 times larger in the film than in the solution. However, in contrast to **2**, complex **5** displays similar efficiencies in both media (0.71 vs 0.66) and similar ratios between the rate constants. The emission wavelength of **5** (552 nm) is red-shifted relative to that of Ir{κ^2-*C*,*N*-[C_6H_4-py]}$_2$(acac) (516 nm).[23]

CONCLUDING REMARKS

This study has revealed that the new organic precursor 2-phenyl-6-(1-phenyl-1-(pyridin-2-yl)ethyl)pyridine allows access to iridium(III) complexes, which are efficient blue-green and green emitters of classes [6tt+1m+2m] and [6tt+3b]. They are prepared starting from the [Ir(μ-Cl)(η^4-COD)]$_2$ dimer by fine-tuning the reaction conditions, in particular the solvent, because primary alcohols carbonylate the metal center and secondary ones must have a high boiling point to perform the *ortho*-C−H bond activation of the phenyl groups of the proligand. The designed ligand imposes a mutually *cis* disposition of the two pyridine units around the metal center, which is in contrast to that generally observed for compounds bearing two orthometalated 2-phenylpyridines. The new emitters display short lifetimes (1.1−4.5 μs) and high quantum yields (0.87−0.54), particularly in PMMA (0.87 and 0.71).

EXPERIMENTAL SECTION

The general information about the experiments and the instrumentation is given in the Supporting Information. [Ir(μ-Cl)(η^4-COD)]$_2$ (**1**),[24] 2-(1-phenylethyl)pyridine,[17] and 2-fluoro-6-phenylpyridine[25] were obtained from published methods. In the NMR spectra (Figures S13−S20), chemical shifts (parts per million) are referenced to residual solvent peaks. Coupling constants (J) are given in hertz.

Synthesis of 2-Phenyl-6-(1-phenyl-1-(pyridin-2-yl)ethyl)-pyridine (H_2L). Oven-dried LiCl (1.4 g, 33.02 mmol) was added to a solution of 2-(1-phenylethyl)pyridine (1 g, 5.46 mmol) in THF (20 mL), under argon, which was cooled to −30 °C. Then, LDA (2 M, 3.55 mL, 7.10 mmol) was added dropwise over 10 min. The reaction mixture was stirred at −30 °C for 1 h. After that, 2-fluoro-6-phenylpyridine (0.95 g, 5.48 mmol) in THF (10 mL) was added

Table 3. Emission Data for 2 and 5

complex	calcd λ_{em} (nm)	media [T (K)]	λ_{em} (nm)	τ (μs)	Φ	k_r[a] (s^{-1})	k_{nr}[b] (s^{-1})	k_r/k_{nr}
2		PMMA (298)	474, 502	1.1	0.87	7.6×10^5	1.1×10^5	6.9
	484	MeTHF (298)	478, 508, 541	2.0	0.54	2.7×10^5	2.3×10^5	1.2
		MeTHF (77)	468, 503, 534 (sh)	2.9				
5		PMMA (298)	551	2.2	0.71	3.3×10^5	1.4×10^5	2.4
	526	MeTHF (298)	552	2.3	0.66	2.8×10^5	1.4×10^5	2.0
		MeTHF (77)	527, 562	4.5				

[a] $k_r = \Phi/\tau$. [b] $k_{nr} = (1 - \Phi)/\tau$.

https://dx.doi.org/10.1021/acs.inorgchem.0c01377
Inorg. Chem. XXXX, XXX, XXX−XXX

dropwise over 5 min. The reaction mixture was stirred at −30 °C for 30 min, warmed to room temperature, and heated to 70 °C for 10 h. The reaction mixture was cooled to room temperature, quenched with saturated NH_4Cl(aq), and extracted with EtOAc. The combined organic fractions were dried with $MgSO_4$ and concentrated. The residual was purified through silica gel column chromatography and eluted with 0−10% EtOAc/hexane. The pure fractions were combined to give 2-phenyl-6-(1-phenyl-1-(pyridin-2-yl)ethyl)pyridine (0.92 g, 50%) as a white solid. ^{1}H NMR (300 MHz, CD_2Cl_2, 298 K): δ 8.59 (m, 1H), 7.98 (m, 2H), 7.70−7.57 (m, 3H), 7.48−7.35 (m, 3H), 7.35−7.20 (m, 3H), 7.17 (m, 4H), 7.07 (m, 1H), 2.37 (s, 3H). ^{13}C NMR (75 MHz, CD_2Cl_2, 298 K): δ 167.4, 166.5, 156.0 (all C_q), 149.2 (CH), 148.9, 140.1 (both C_q), 137.2, 136.2, 129.4 (all CH), 129.3 (2CH), 129.1 (2CH), 128.5 (2CH), 127.3 (2CH), 126.7, 124.2, 122.7, 121.7, 118.0 (all CH), 58.5 (C_q), 28.7 (CH_3).

Preparation of Ir(κ^4-*C,C′,N,N′*-L)Cl(CO) (2). Complex **1** (300 mg, 0.447 mmol) and H_2L (300 mg, 0.894 mmol) in 5 mL of 2-ethoxyethanol were heated at reflux for 24 h. Then, a pale yellow solid appeared. The suspension was decanted, and the solid was washed with methanol (3 × 5 mL) and dried under vacuum. Yield: 310 mg (59%). Crystals of **2**, suitable for X-ray diffraction analysis, were obtained at 4 °C by slow diffusion of pentane into a dichloromethane solution of the complex. Anal. Calcd for $C_{25}H_{18}ClIrN_2O$: C, 50.89; H, 3.07; N, 4.75. Found: C, 50.51; H, 3.16; N, 4.58. HRMS (electrospray, *m*/*z*): calcd for $C_{25}H_{18}IrN_2O$ $[M - Cl]^+$ 555.1044, found 555.1141. T_{d5} = 370 °C (Figure S21).[26] IR (cm^{-1}): ν(CO) 2011 (s). ^{1}H NMR (400 MHz, CD_2Cl_2, 298 K): δ 9.31 (d, 1H, *J* = 5.3 Hz, CH py), 8.02 (dd, 1H, *J* = 7.5, 0.8 Hz, CH Ph), 8.00−7.92 (m, 2H, CH py), 7.85 (t, 1H, *J* = 8.0 Hz, CH py), 7.72 (dd, 1H, *J* = 7.4, 1.4 Hz, CH Ph), 7.68 (dd, 1H, *J* = 7.5, 0.8 Hz), 7.64 (dd, 1H, *J* = 7.7, 1.3 Hz), 7.51 (dd, 1H, *J* = 7.9, 0.8 Hz, CH Py), 7.36 (dd, 1H, *J* = 8.0, 1.2 Hz, CH Ph), 7.29 (ddd, 1H, *J* = 7.2, 5.6, 1.8 Hz, CH py), 7.24 (ddd, 1H, *J* = 7.5, 7.5, 1.4 Hz, CH Ph), 7.11 (ddd, 1H, *J* = 7.5, 7.5, 1.2 Hz, CH Ph), 6.97 (ddd, 1H, *J* = 7.6, 7.6, 1.5 Hz, CH Ph), 6.82 (ddd, 1H, *J* = 7.3, 7.3, 1.3 Hz, CH Ph), 2.63 (s, 3H, CH_3). ^{13}C{^{1}H} NMR (100.63 MHz, CD_2Cl_2, 298 K): δ 172.4 (CO), 167.1 (C_q py), 158.1 (C_q py), 157.4 (C_q py), 157.3 (CH py), 150.5 (C_q Ph), 145.1 (Ir−C_q Ph), 140.4 (2CH py), 139.6 (CH Ph), 138.6 (C_q Ph), 137.2 (CH Ph), 133.7 (Ir-C_q Ph), 131.1 (CH Ph), 127.3 (CH Ph), 125.2 (CH Ph), 125.0 (CH Ph), 124.8 (CH py), 124.6 (CH Ph), 123.8 (CH Ph), 122.1 (CH py), 118.0 (CH py), 117.9 (CH py), 59.8 (C_q), 22.6 (CH_3).

Reaction of 1 with H_2L in Propan-2-ol under Reflux: Formation of [Ir(κ^2-*N,N′*-H_2L)(η^4-COD)][$IrCl_2$(η^4-COD)] (3). Complex **1** (200 mg, 0.298 mmol) and H_2L (200 mg, 0.596 mmol) in 5 mL of isopropanol were heated under reflux for 24 h. Then, a solid precipitated. The resulting suspension was decanted, and the orange solid was washed with methanol (3 × 5 mL) and dried under vacuum. Yield: 159.2 mg (53%). Crystals of **3**, suitable for X-ray diffraction analysis, were obtained at 4 °C by slow diffusion of pentane into a dichloromethane solution of the salt. Anal. Calcd for $C_{40}H_{44}Cl_2Ir_2N_2$: C, 47.66; H, 4.40; N, 2.78. Found: C, 47.31; H, 4.01; N, 2.59. HRMS (electrospray, *m*/*z*): calcd for $C_{32}H_{32}IrN_2$ $[M]^+$ 637.2191, found 637.2168; calcd for $C_8H_{12}IrCl_2$ $[M]^-$ 370.9936, found 370.9941. The ^{1}H NMR spectrum in a CD_2Cl_2 solution shows an exchange of H_2L between the two Ir(η^4-COD) moieties of the salt, even at 193 K (Figures S17 and S18).

Preparation of [Ir(μ-Cl)(κ^4-*C,C′,N,N′*-L)]$_2$ (4). Complex **1** (200 mg, 0.298 mmol) and H_2L (200 mg, 0.596 mmol) in 5 mL of 1-phenylethanol were heated at 140 °C for 48 h. Then, the starting red solution became very dark red. The resulting solution was evaporated under vacuum until it was almost dry, and 5 mL of MeOH was added. An orange solid appeared, which was treated with dichloromethane until the mother liquors were colorless and dried under vacuum. Yield: 60.3 mg (18%). Anal. Calcd for $C_{48}H_{36}Cl_2Ir_2N_4$: C, 51.28; H, 3.23; N, 4.98. Found: C, 50.91; H, 3.52; N, 4.92. MALDI-TOF (*m*/*z*): calcd for $C_{24}H_{18}IrClN_2$ $[M/2]^+$ 562.1, found 562.0.

Preparation of Ir(κ^4-*C,C′,N,N′*-L)(acac) (5). Complex **1** (200 mg, 0.298 mmol) and H_2L (200 mg, 0.596 mmol) in 5 mL of 1-phenylethanol were heated at 140 °C for 48 h. After this time, the starting red solution became very dark red. The resulting solution was evaporated under vacuum until it was almost dry, and 5 mL of methanol was added. An orange solid appeared, which was washed with methanol (3 × 5 mL) and dried under vacuum (168 mg). Acetylacetone (153 μL, 1.49 mmol) and KOH (98 mg, 1.49 mmol) in 2 mL of methanol were added to a solution of the orange solid (168 mg) in 15 mL of tetrahydrofuran, and the mixture was stirred at 60 °C for 90 min. The solvent was removed under vacuum. The resulting residue was treated with 15 mL of dichloromethane, and the suspension filtered off to afford an orange solution, which was concentrated under vacuum. The addition of 5 mL of pentane led to a yellowish orange solid, which was washed with 2 × 4 mL of pentane and dried under vacuum. The solid was purified by silica column chromatography using toluene with a gradual increase in the amount of dichloromethane as the eluent, until a 1:1 toluene:dichloromethane ratio was achieved. Yield: 128 mg (34%). Crystals of **5**, suitable for X-ray diffraction analysis, were obtained at 4 °C by slow diffusion of pentane into a dichloromethane solution of the complex. Anal. Calcd for $C_{29}H_{25}IrN_2O_2$: C, 55.66; H, 4.03; N, 4.48. Found: C, 55.33; H, 4.38; N, 4.21. HRMS (electrospray, *m*/*z*): calcd for $C_{29}H_{25}IrNaN_2O_2$ $[M + Na]^+$ 649.1439, found 649.1447. T_{d5} = 334 °C (Figure S21).[26] IR (cm^{-1}): ν(C=O) 1580 (s), 1514 (s). ^{1}H NMR (400.13 MHz, CD_2Cl_2, 298 K): δ 8.24 (ddd, *J* = 5.5, 1.7, 0.9 Hz, 1H), 7.88−7.77 (m, 2H), 7.62−7.55 (m, 2H), 7.54−7.50 (m, 2H), 7.48−7.44 (m, 1H), 7.34 (dd, *J* = 7.8, 1.2 Hz, 1H), 7.27−7.19 (m, 2H), 7.10 (ddd, *J* = 7.2, 7.2, 1.3 Hz, 1H), 6.98 (ddd, *J* = 7.3, 7.3, 1.3 Hz, 1H), 6.83−6.72 (m, 2H), 5.44 (s, 1H, CH acac), 2.59 (s, 3H, Me L), 2.16, 1.53 (both s, 3H each, Me acac). ^{13}C{^{1}H} NMR (100.63 MHz, CD_2Cl_2, 298 K): δ 185.0, 184.9 (both CO acac), 170.8, 160.8, 160.6, 160.5 (all C_q), 151.8 (CH), 164.9, 139.7, 138.2 (all C_q), 137.9, 136.9, 136.3, 134.2, 128.4, 125.5, 124.5, 124.0 (all CH), 122.9 (2 CH), 122.2, 121.6, 117.0, 116.0 (all CH), 101.4 (CH acac), 59.1 (C_qMe L), 28.5, 28.3 (both Me acac), 22.8 (Me L).

■ ASSOCIATED CONTENT

Supporting Information

The Supporting Information is available free of charge at https://pubs.acs.org/doi/10.1021/acs.inorgchem.0c01377.

General information for the Experimental Section, structural analysis, computational details and energies of optimized structures, experimental and computed UV−vis spectra, cyclic voltammograms, frontier orbitals, natural transition orbitals, normalized excitation and emission spectra, NMR spectra, and thermogravimetric analysis curves (PDF)

Cartesian coordinates of the optimized structures (XYZ)

Accession Codes

CCDC 1998438−1998440 contain the supplementary crystallographic data for this paper. These data can be obtained free of charge via www.ccdc.cam.ac.uk/data_request/cif, or by emailing data_request@ccdc.cam.ac.uk, or by contacting The Cambridge Crystallographic Data Centre, 12 Union Road, Cambridge CB2 1EZ, UK; fax: +44 1223 336033.

■ AUTHOR INFORMATION

Corresponding Author

Miguel A. Esteruelas − *Departamento de Química Inorgánica, Instituto de Síntesis Química y Catálisis Homogénea (ISQCH), Centro de Innovación en Química Avanzada (ORFEO-CINQA), Universidad de Zaragoza-CSIC, 50009 Zaragoza, Spain;* orcid.org/0000-0002-4829-7590; Email: maester@unizar.es

Authors

Llorenç Benavent − *Departamento de Química Inorgánica, Instituto de Síntesis Química y Catálisis Homogénea (ISQCH),*

https://dx.doi.org/10.1021/acs.inorgchem.0c01377
Inorg. Chem. XXXX, XXX, XXX−XXX

Centro de Innovación en Química Avanzada (ORFEO-CINQA), Universidad de Zaragoza-CSIC, 50009 Zaragoza, Spain

Pierre-Luc T. Boudreault − *Universal Display Corporation, Ewing, New Jersey 08618, United States*

Ana M. López − *Departamento de Química Inorgánica, Instituto de Síntesis Química y Catálisis Homogénea (ISQCH), Centro de Innovación en Química Avanzada (ORFEO-CINQA), Universidad de Zaragoza-CSIC, 50009 Zaragoza, Spain;* orcid.org/0000-0001-7183-4975

Enrique Oñate − *Departamento de Química Inorgánica, Instituto de Síntesis Química y Catálisis Homogénea (ISQCH), Centro de Innovación en Química Avanzada (ORFEO-CINQA), Universidad de Zaragoza-CSIC, 50009 Zaragoza, Spain;* orcid.org/0000-0003-2094-719X

Jui-Yi Tsai − *Universal Display Corporation, Ewing, New Jersey 08618, United States;* orcid.org/0000-0002-8516-9985

Complete contact information is available at: https://pubs.acs.org/10.1021/acs.inorgchem.0c01377

Notes

The authors declare no competing financial interest.

■ ACKNOWLEDGMENTS

Financial support from the MINECO of Spain [Projects CTQ2017-82935-P (AEI/FEDER, UE) and RED2018-102387-T], Gobierno de Aragón (Group E06_20R and Project LMP148_18), FEDER, and the European Social Fund is acknowledged. The BIFI Institute and CESGA Supercomputing Center are also acknowledged for technical support and the use of computational resources.

■ REFERENCES

(1) Powell, B. J. Theories of phosphorescence in organo-transition metal complexes - From relativistic effects to simple models and design principles for organic light-emitting diodes. *Coord. Chem. Rev.* **2015**, *295*, 46−79.

(2) Yersin, H.; Rausch, A. F.; Czerwieniec, R.; Hofbeck, T.; Fischer, T. The triplet state of organo-transition metal compounds. Triplet harvesting and singlet harvesting for efficient OLEDs. *Coord. Chem. Rev.* **2011**, *255*, 2622−2652.

(3) See for example: (a) You, Y.; Nam, W. Photofunctional triplet excited states of cyclometalated Ir(III) complexes: beyond electroluminescence. *Chem. Soc. Rev.* **2012**, *41*, 7061−7084. (b) Zanoni, K. P. S.; Coppo, R. L.; Amaral, R. C.; Murakami Iha, N. Y. Ir(III) complexes designed for light-emitting devices: beyond the luminescence color array. *Dalton Trans.* **2015**, *44*, 14559−14573. (c) Omae, I. Application of the five-membered ring blue light-emitting iridium products of cyclometalation reactions as OLEDs. *Coord. Chem. Rev.* **2016**, *310*, 154−169. (d) Henwood, A. F.; Zysman-Colman, E. Lessons learned in tuning the optoelectronic properties of phosphorescent iridium(III) complexes. *Chem. Commun.* **2017**, *53*, 807−826. (e) Li, T.-Y.; Wu, J.; Wu, Z.-G.; Zheng, Y.-X.; Zuo, J.-L.; Pan, Y. Rational design of phosphorescent iridium(III) complexes for emission color tunability and their applications in OLEDs. *Coord. Chem. Rev.* **2018**, *374*, 55−92. (f) Lee, S.; Han, W.-S. Cyclometalated Ir(III) complexes towards blue-emissive dopant for organic light-emitting diodes: fundamentals of photophysics and designing strategies. *Inorg. Chem. Front.* **2020**, *7*, 2396.

(4) See for example: (a) Esteruelas, M. A.; Gómez-Bautista, D.; López, A. M.; Oñate, E.; Tsai, J.-Y.; Xia, C. η^1-Arene Complexes as Intermediates in the Preparation of Molecular Phosphorescent Iridium(III) Complexes. *Chem. - Eur. J.* **2017**, *23*, 15729−15737. (b) Esteruelas, M. A.; Oñate, E.; Palacios, A. U. Selective Synthesis and Photophysical Properties of Phosphorescent Heteroleptic Iridium(III) Complexes with Two Different Bidentate Groups and Two Different Monodentate Ligands. *Organometallics* **2017**, *36*, 1743−1755. (c) Benjamin, H.; Liang, J.; Liu, Y.; Geng, Y.; Liu, X.; Zhu, D.; Batsanov, A. S.; Bryce, M. R. Color Tuning of Efficient Electroluminescence in the Blue and Green Regions Using Heteroleptic Iridium Complexes with 2-Phenoxyoxazole Ancillary Ligands. *Organometallics* **2017**, *36*, 1810−1821. (d) Davidson, R.; Hsu, Y.-T.; Bhagani, C.; Yufit, D.; Beeby, A. Exploring the Chemistry and Photophysics of Substituted Picolinates Positional Isomers in Iridium(III) Bisphenylpyridine Complexes. *Organometallics* **2017**, *36*, 2727−2735. (e) Leopold, H.; Císařová, I.; Strassner, T. Phosphorescent C^C* Cyclometalated Thiazol-2-ylidene Iridium(III) Complexes: Synthesis, Structure, and Photophysics. *Organometallics* **2017**, *36*, 3016−3018. (f) Matteucci, E.; Monti, F.; Mazzoni, R.; Baschieri, A.; Bizzarri, C.; Sambri, L. Click-Derived Triazolylidenes as Chelating Ligands: Achievement of a Neutral and Luminescent Iridium(III)-Triazolide Complex. *Inorg. Chem.* **2018**, *57*, 11673−11686. (g) Lai, P.-N.; Brysacz, C. H.; Alam, K. M.; Ayoub, N. A.; Gray, T. G.; Bao, J.; Teets, T. S. Highly Efficient Red-Emitting Bis-Cyclometalated Iridium Complexes. *J. Am. Chem. Soc.* **2018**, *140*, 10198−10207. (h) Ma, X.-F.; Luo, X.-F.; Yan, Z.-P.; Wu, Z.-G.; Zhao, Y.; Zheng, Y.-X.; Zuo, J.-L. Syntheses, Crystal Structures, and Photoluminescence of a Series of Iridium(III) Complexes Containing the Pentafluorosulfanyl Group. *Organometallics* **2019**, *38*, 3553−3559. (i) Na, H.; Cañada, L. M.; Wen, Z.; I-Chia Wu, J.; Teets, T. S. Mixed-carbene cyclometalated iridium complexes with saturated blue luminescence. *Chem. Sci.* **2019**, *10*, 6254−6260. (j) Adamovich, V.; Boudreault, P.-L. T.; Esteruelas, M. A.; Gómez-Bautista, D.; López, A. M.; Oñate, E.; Tsai, J.-Y. Preparation via a NHC Dimer Complex, Photophysical Properties, and Device Performance of Heteroleptic Bis(Tridentate) Iridium(III) Emitters. *Organometallics* **2019**, *38*, 2738−2747. (k) Castro-Rodrigo, R.; Esteruelas, M. A.; Gómez-Bautista, D.; Lezáun, V.; López, A. M.; Oliván, M.; Oñate, E. Influence of the Bite Angle of Dianionic C,N,C-Pincer Ligands on the Chemical and Photophysical Properties of Iridium(III) and Osmium(IV) Hydride Complexes. *Organometallics* **2019**, *38*, 3707−3718. (l) Boudreault, P.-L. T.; Esteruelas, M. A.; Gómez-Bautista, D.; Izquierdo, S.; López, A. M.; Oñate, E.; Raga, E.; Tsai, J.-Y. Preparation and Photophysical Properties of *Bis*(tridentate) Iridium(III) Emitters: Pincer Coordination of 2,6-Di(2-pyridyl)-phenyl. *Inorg. Chem.* **2020**, *59*, 3838−3849.

(5) See for example: (a) Kim, T.; Kim, H.; Lee, K. M.; Lee, Y. S.; Lee, M. H. Phosphorescence Color Tuning of Cyclometalated Iridium Complexes by *o*-Carborane Substitution. *Inorg. Chem.* **2013**, *52*, 160−168. (b) Lee, Y. H.; Park, J.; Jo, S.-J.; Kim, M.; Lee, J.; Lee, S. U.; Lee, M. H. Manipulation of Phosphorescence Efficiency of Cyclometalated Iridium Complexes by Substituted *o*-Carboranes. *Chem. - Eur. J.* **2015**, *21*, 2052−2061. (c) Liu, C.; Lv, X.; Xing, Y.; Qiu, J. Trifluoromethyl-substituted cyclometalated iridium^{III} emitters with high photostability for continuous oxygen sensing. *J. Mater. Chem. C* **2015**, *3*, 8010−8017. (d) Pal, A. K.; Henwood, A. F.; Cordes, D. B.; Slawin, A. M. Z.; Samuel, I. D. W.; Zysman-Colman, E. Blue-to-Green Emitting Neutral Ir(III) Complexes Bearing Pentafluorosulfanyl Groups: A Combined Experimental and Theoretical Study. *Inorg. Chem.* **2017**, *56*, 7533−7544. (e) Boudreault, P.-L. T.; Esteruelas, M. A.; Mora, E.; Oñate, E.; Tsai, J.-Y. Pyridyl-Directed C-H and C-Br Bond Activations Promoted by Dimer Iridium-Olefin Complexes. *Organometallics* **2018**, *37*, 3770−3779.

(6) See for example: (a) Ionkin, A. S.; Marshall, W. J.; Roe, D. C.; Wang, Y. Synthesis, structural characterization and the first electroluminescent properties of tris- and bis-cycloiridiated complexes of sterically hindered electron-poor 2-(3,5-bis(trifluoromethyl)phenyl)-4-trifluoromethylpyridine. *Dalton Trans.* **2006**, 2468−2478. (b) Yuan, X.; Zhang, S.; Ding, Y. Isolation, characterization and photophysical properties of a 2-(4,6-difluorophenyl)pyridyl iridium(III) methoxide dimeric complex. *Inorg. Chem. Commun.* **2012**, *17*, 26−29. (c) Gupta, S. K.; Haridas, A.; Choudhury, J. Remote Terpyridine Integrated NHC-Ir^{III} luminophores as Potential Dual-Emissive Ratiometric O_2 Probes. *Chem. - Eur. J.* **2017**, *23*, 4770−4773.

(7) (a) Wilkinson, A. J.; Puschmann, H.; Howard, J. A. K.; Foster, C. E.; Williams, J. A. G. Luminescent Complexes of Iridium(III) Containing N^C^N-Coordinating Terdentate Ligands. *Inorg. Chem.* **2006**, *45*, 8685−8699. (b) Chen, J.-L.; Wu, Y.-H.; He, L.-H.; Wen, H.-R.; Liao, J.; Hong, R. Iridium(III) Bis-tridentate Complexes with 6-(5-Trifluoromethylpyrazol-3-yl)-2,2′-bipyridine Chelating Ligands: Synthesis, Characterization, Photophysical Properties. *Organometallics* **2010**, *29*, 2882−2891. (c) Tong, B.; Ku, H.-Y.; Chen, I.-J.; Chi, Y.; Kao, H.-C.; Yeh, C.-C.; Chang, C.-H.; Liu, S.-H.; Lee, G.-H.; Chou, P.-T. Heteroleptic Ir(III) phosphors with bis-tridentate chelating architecture for high efficiency OLEDs. *J. Mater. Chem. C* **2015**, *3*, 3460−3471. (d) Lu, C.-W.; Wang, Y.; Chi, Y. Metal Complexes with Azolate-Functionalized Multidentate Ligands: Tactical Designs and Optoelectronic Applications. *Chem. - Eur. J.* **2016**, *22*, 17892−17908. (e) Kuei, C.-Y.; Tsai, W.-L.; Tong, B.; Jiao, M.; Lee, W.-K.; Chi, Y.; Wu, C.-C.; Liu, S.-H.; Lee, G.-H.; Chou, P.-T. Bis-Tridentate Ir(III) Complexes with Nearly Unitary RGB Phosphorescence and Organic Light-Emitting Diodes with External Quantum Efficiency Exceeding 31%. *Adv. Mater.* **2016**, *28*, 2795−2800. (f) Lin, J.; Chau, N.-Y.; Liao, J.-L.; Wong, W.-Y.; Lu, C.-Y.; Sie, Z.-T.; Chang, C.-H.; Fox, M. A.; Low, P. J.; Lee, G.-H.; Chi, Y. Bis-Tridentate Iridium(III) Phosphors Bearing Functional 2-Phenyl-6-(imidazol-2-ylidene)pyridine and 2-(Pyrazol-3-yl)-6-phenylpyridine Chelates for Efficient OLEDs. *Organometallics* **2016**, *35*, 1813−1824. (g) Kuo, H.-H.; Chen, Y.-T.; Devereux, L. R.; Wu, C. C.; Fox, M. A.; Kuei, C.-Y.; Chi, Y.; Lee, G.-H. Bis-Tridentate Ir(III) Metal Phosphors for Efficient Deep-Blue Organic Light-Emitting Diodes. *Adv. Mater.* **2017**, *29*, 1702464. (h) Lin, J.; Wang, Y.; Gnanasekaran, P.; Chiang, Y.-C.; Yang, C.-C.; Chang, C.-H.; Liu, S.-H.; Lee, G.-H.; Chou, P.-T.; Chi, Y.; Liu, S.-W. Unprecedented Homoleptic Bis-Tridentate Iridium(III) Phosphors: Facile, Scaled-Up Production, and Superior Chemical Stability. *Adv. Funct. Mater.* **2017**, *27*, 1702856. (i) Hsu, L.-Y.; Liang, Q.; Wang, Z.; Kuo, H.-H.; Tai, W.-S.; Su, S.-J.; Zhou, X.; Yuan, Y.; Chi, Y. Bis-tridentate Ir^{III} Phosphors Bearing Two Fused Five-Six-Membered Metallacycles: A Strategy to Improved Photostability of Blue Emitters. *Chem. - Eur. J.* **2019**, *25*, 15375−15386. (j) Gnanasekaran, P.; Yuan, Y.; Lee, C.-S.; Zhou, X.; Jen, A. K.-Y.; Chi, Y. Realization of Highly Efficient Red Phosphorescence from Bis-Tridentate Iridium(III) Phosphors. *Inorg. Chem.* **2019**, *58*, 10944−10954.

(8) (a) Williams, J. A. G.; Wilkinson, A. J.; Whittle, V. L. Light-emitting iridium complexes with tridentate ligands. *Dalton Trans.* **2008**, 2081−2099. (b) Kuei, C.-Y.; Liu, S.-H.; Chou, P.-T.; Lee, G.-H.; Chi, Y. Room temperature blue phosphorescence: a combined experimental and theoretical study on the bis-tridentate Ir(III) metal complexes. *Dalton Trans.* **2016**, *45*, 15364−15373. (c) Williams, J. A. G. The coordination chemistry of dipyridylbenzene: N-deficient terpyridine or panacea for brightly luminescent metal complexes? *Chem. Soc. Rev.* **2009**, *38*, 1783−1801. (d) Chi, Y.; Chang, T.-K.; Ganesan, P.; Rajakannu, P. Emissive bis-tridentate Ir(III) metal complexes: Tactics, photophysics and applications. *Coord. Chem. Rev.* **2017**, *346*, 91−100. (e) Kuo, H.-H.; Zhu, Z.-L.; Lee, C.-S.; Chen, Y.-K.; Liu, S.-H.; Chou, P.-T.; Jen, A. K.-Y.; Chi, Y. Bis-Tridentate Iridium(III) Phosphors with Very High Photostability and Fabrication of Blue-Emitting OLEDs. *Adv. Sci.* **2018**, *5*, 1800846.

(9) (a) Vezzu, D. A. K.; Deaton, J. C.; Jones, J. S.; Bartolotti, L.; Harris, C. F.; Marchetti, A. P.; Kondakova, M.; Pike, R. D.; Huo, S. Highly Luminescent Tetradentate Bis-Cyclometalated Platinum Complexes: Design, Synthesis, Structure, Photophysics, and Electroluminescence Application. *Inorg. Chem.* **2010**, *49*, 5107−5119. (b) Huo, S.; Harris, C. F.; Vezzu, D. A. K.; Gagnier, J. P.; Smith, M. E.; Pike, R. D.; Li, Y. Novel phosphorescent tetradentate bis-cyclometalated ĈC*N̂N-coordinated platinum complexes: structure, photophysics, and a synthetic adventure. *Polyhedron* **2013**, *52*, 1030−1040. (c) Huo, S.; Carroll, J.; Vezzu, D. A. K. Design, Synthesis and Applications of Highly Phosphorescent Cyclometalated Platinum complexes. *Asian J. Org. Chem.* **2015**, *4*, 1210−1245. (d) Fleetham, T. B.; Huang, L.; Klimes, K.; Brooks, J.; Li, J. Tetradentate Pt(II) Complexes with 6-Membered Chelate Rings: A New Route for Stable and Efficient Blue OLEDs. *Chem. Mater.* **2016**, *28*, 3276−3282. (e) Wang, X.; Peng, T.; Nguyen, C.; Lu, Z.-H.; Wang, N.; Wu, W.; Li, Q.; Wang, S. Highly Efficient Deep-Blue Electrophosphorescent Pt(II) Compounds with Non-Distorted Flat Geometry: Tetradentate versus Macrocyclic Chelate Ligands. *Adv. Funct. Mater.* **2017**, *27*, 1604318. (f) Lee, C.-H.; Tang, M.-C.; Kong, F. K.-W.; Cheung, W.-L.; Ng, M.; Chan, M.-Y.; Yam, V. W.-W. Isomeric Tetradentate Ligand-Containing Cyclometalated Gold(III) Complexes. *J. Am. Chem. Soc.* **2020**, *142*, 520−529. (g) Li, G.; Zhan, F.; Zheng, J.; Yang, Y.-F.; Wang, Q.; Chen, Q.; Shen, G.; She, Y. Highly Efficient Phosphorescent Tetradentate Platinum (II) Complexes Containing Fused 6/5/6 Metallocycles. *Inorg. Chem.* **2020**, *59*, 3718−3729.

(10) (a) Chow, P.-K.; Ma, C.; To, W.-P.; Tong, G. S. M.; Lai, S.-L.; Kui, S. C. F.; Kwok, W.-M.; Che, C.-M. Strongly Phosphorescent Palladium(II) Complexes of Tetradentate Ligands with Mixed Oxygen, Carbon, and Nitrogen Donor Atoms: Photphysics, Photochemistry, and Applications. *Angew. Chem., Int. Ed.* **2013**, *52*, 11775−11779. (b) Zhu, Z.-Q.; Fleetham, T.; Turner, E.; Li, J. Harvesting All Electrogenerated Excitons through Metal Assisted Delayed Fluorescent Materials. *Adv. Mater.* **2015**, *27*, 2533−2537. (c) Chow, P.-K.; Cheng, G.; Tong, G. S. M.; Ma, C.; Kwok, W.-M.; Ang, W.-H.; Chung, C. Y.-S.; Yang, C.; Wang, F.; Che, C.-M. Highly luminescent palladium(II) complexes with sub-millisecond blue to green phosphorescent excited states. Photocatalysis and highly efficient PSF-OLEDs. *Chem. Sci.* **2016**, *7*, 6083−6098. (d) Zhu, Z.-Q.; Park, C.-D.; Klimes, K.; Li, J. Highly Efficient Blue OLEDs Based on Metal-Assisted Delayed Fluorescence Pd(II) Complexes. *Adv. Opt. Mater.* **2019**, *7*, 1801518.

(11) (a) Palmer, J. H.; Durrell, A. C.; Gross, Z.; Winkler, J. R.; Gray, H. B. Near-IR Phosphorescence of Iridium (III) Corroles at Ambient Temperature. *J. Am. Chem. Soc.* **2010**, *132*, 9230−9231. (b) Koren, K.; Borisov, S. M.; Saf, R.; Klimant, I. Strongly Phosphorescent Iridium(III)-Porphyrins - New Oxygen Indicators with Tuneable Photophysical Properties and Functionalities. *Eur. J. Inorg. Chem.* **2011**, *2011*, 1531−1534. (c) Palmer, J. H.; Brock-Nannestad, T.; Mahammed, A.; Durrell, A. C.; VanderVelde, D.; Virgil, S.; Gross, Z.; Gray, H. B. Nitrogen Insertion into a Corrole Ring: Iridium Monoazaporphyrins. *Angew. Chem., Int. Ed.* **2011**, *50*, 9433−9436. (d) Sinha, W.; Ravotto, L.; Ceroni, P.; Kar, S. NIR-emissive iridium(III) corrole complexes as efficient singlet oxygen sensitizers. *Dalton Trans.* **2015**, *44*, 17767−17773. (e) Chen, W.; Zhang, J.; Mack, J.; Kubheka, G.; Nyokong, T.; Shen, Z. Corrole-BODIPY conjugates: enhancing the fluorescence and phosphorescence of the corrole complex *via* efficient through bond energy transfer. *RSC Adv.* **2015**, *5*, 50962−50967. (f) Maurya, Y. K.; Ishikawa, T.; Kawabe, Y.; Ishida, M.; Toganoh, M.; Mori, S.; Yasutake, Y.; Fukatsu, S.; Furuta, H. Near-Infrared Phosphorescent Iridium(III) Benzonorrole Complexes Possessing Pyridine-based Axial Ligands. *Inorg. Chem.* **2016**, *55*, 6223−6230. (g) Chen, D.; Li, K.; Guan, X.; Cheng, G.; Yang, C.; Che, C.-M. Luminescent Iridium(III) Complexes Supported by a Tetradentate Trianionic Ligand Scaffold with Mixed O, N, and C Donor Atoms: Synthesis, Structures, Photophysical Properties, and Material Applications. *Organometallics* **2017**, *36*, 1331−1344.

(12) The metal center is better encapsulated with this coordination, which appears to favor narrow and bluer emissions. This, which is highly desirable for OLED display applications, seems to be related to less pronounced differences between the excited-state structure and the ground-state structure. See: (a) Alabau, R. G.; Esteruelas, M. A.; Oliván, M.; Oñate, E.; Palacios, A. U.; Tsai, J.-Y.; Xia, C. Osmium(II) Complexes Containing a Dianionic CCCC-Donor Tetradentate Ligand. *Organometallics* **2016**, *35*, 3981−3995.

(13) Lee, Y. H.; Park, J.; Lee, J.; Lee, S. U.; Lee, M. H. Impact of Restricted Rotation of *o*-Carborane on Phosphorescence Efficiency. *J. Am. Chem. Soc.* **2015**, *137*, 8018−8021.

(14) Bünzli, A. M.; Pertegás, A.; Momblona, C.; Junquera-Hernández, J. M.; Constable, E. C.; Bolink, H. J.; Ortí, E.; Housecroft, C. E. $[Ir(C^N)_2(N^N)]^+$ emitters containing a naphthalene unit within a linker between the two cyclometallating ligands. *Dalton Trans.* **2016**, *45*, 16379−16392.

https://dx.doi.org/10.1021/acs.inorgchem.0c01377
Inorg. Chem. XXXX, XXX, XXX−XXX

(15) Li, Y.-S.; Liao, J.-L.; Lin, K.-T.; Hung, W.-Y.; Liu, S.-H.; Lee, G.-H.; Chou, P.-T.; Chi, Y. Sky Blue-Emitting Iridium (III) Complexes Bearing Nonplanar Tetradentate Chromophore and Bidentate Ancillary. *Inorg. Chem.* **2017**, *56*, 10054−10060.
(16) Esteruelas, M. A.; López, A. M.; Oñate, E.; San-Torcuato, A.; Tsai, J.-Y.; Xia, C. Preparation of Phosphorescent Iridium(III) Complexes with a Dianionic C,C,C,C-Tetradentate Ligand. *Inorg. Chem.* **2018**, *57*, 3720−3730.
(17) Yuan, Y.; Gnanasekaran, P.; Chen, Y.-W.; Lee, G.-H.; Ni, S.-F.; Lee, C.-S.; Chi, Y. Iridium(III) Complexes Bearing a Formal Tetradentate Coordination Chelate: Structural Properties and Phosphorescence Fine-Tuned by Ancillaries. *Inorg. Chem.* **2020**, *59*, 523−532.
(18) (a) Friedrich, A.; Schneider, S. Acceptorless Dehydrogenation of Alcohols: Perspectives for Synthesis and H_2 Storage. *ChemCatChem* **2009**, *1*, 72−73. (b) Johnson, T. C.; Morris, D. J.; Wills, M. Hydrogen generation from formic acid and alcohols using homogeneous catalysts. *Chem. Soc. Rev.* **2010**, *39*, 81−88. (c) Trincado, M.; Banerjee, D.; Grützmacher, J. Molecular catalysts for hydrogen production from alcohols. *Energy Environ. Sci.* **2014**, *7*, 2464−2503. (d) Nielsen, M. Hydrogen Production by Homogeneous Catalysis: Alcohol acceptorless dehydrogenation. In *Hydrogen Production and Remediation of Carbon and Pollutants*; Lichtfouse, E., Schwarzbauer, J., Robert, D., Eds.; Springer: Cham, Switzerland, 2015; Chapter 1, pp 1−60.
(19) See, for example: (a) Esteruelas, M. A.; Hernández, Y. A.; López, A. M.; Oliván, M.; Rubio, L. Reactions of a Dihydride-Osmium (IV) Complex with Aldehydes: Influence of the Substituent at the Carbonyl Group. *Organometallics* **2008**, *27*, 799−802. (b) Alós, J.; Esteruelas, M. A.; Oliván, M.; Oñate, E.; Puylaert, P. C-H Bond Activation Reactions in Ketones and Aldehydes Promoted by POP-Pincer Osmium and Ruthenium Complexes. *Organometallics* **2015**, *34*, 4908−4921.
(20) Churchill, M. R.; Bezman, S. A. X-ray Crystallographic Studies on Fluxional Pentacoordinate Transition Metal Complexes. III. (Cycloocta-1,5-diene)[bis(1,3-diphenylphosphino)propane]-methyliridium(I). *Inorg. Chem.* **1973**, *12*, 531−536.
(21) Boudreault, P.-L. T.; Esteruelas, M. A.; Mora, E.; Oñate, E.; Tsai, J.-Y. Suzuki-Miyaura Cross-Coupling Reactions for Increasing the Efficiency of Tris-Heteroleptic Iridium(III) Emitters. *Organometallics* **2019**, *38*, 2883−2887.
(22) Adamovich, V.; Bajo, S.; Boudreault, P.-L.; Esteruelas, M. A.; López, A. M.; Martín, J.; Oliván, M.; Oñate, E.; Palacios, A. U.; San-Torcuato, A.; Tsai, J.-Y.; Xia, C. Preparation of Tris-Heteroleptic Iridium(III) Complexes Containing a Cyclometalated Aryl-N-Heterocyclic Carbene Ligand. *Inorg. Chem.* **2018**, *57*, 10744−10760.
(23) Lamansky, S.; Djurovich, P.; Murphy, D.; Abdel-Razzaq, F.; Kwong, R.; Tsyba, I.; Bortz, M.; Mui, B.; Bau, R.; Thompson, M. E. Synthesis and Characterization of Phosphorescent Cyclometalated Iridium Complexes. *Inorg. Chem.* **2001**, *40*, 1704−1711.
(24) Herde, J. L.; Lambert, J. C.; Senoff, C. V.; Cushing, M. A. Cyclooctene and 1,5-Cyclooctadiene Complexes of Iridium(I). *Inorg. Synth.* **2007**, *15*, 18−20.
(25) Liu, C.; Li, X.; Liu, C.; Wang, X.; Qiu, J. Palladium-catalyzed ligand-free and efficient Suzuki-Miyaura reaction of heteroaryl halides with MIDA boronates in water. *RSC Adv.* **2015**, *5*, 54312−54315.
(26) T_{ds} represents the temperature at which 5% of the initial weight is lost during thermogravimetric analysis.

https://dx.doi.org/10.1021/acs.inorgchem.0c01377
Inorg. Chem. XXXX, XXX, XXX−XXX